

Introduction: The mechanistic target of rapamycin (mTOR) coordinates the growth and metabolism of eukaryotic cells with a central role in the regulation of many fundamental cellular processes. It is strongly connected to phosphatidylinositol 3-kinase (PI3K) and AKT signaling. Activation of the PI3K/AKT/mTOR pathway leads to a profound disruption in the control of cell growth and survival, which ultimately leads to competitive growth advantage, metastatic competence, angiogenesis and therapeutic resistance.

Material and methods: To explore the common competitive adenosine triphosphate (ATP) inhibitors PI3K/AKT and PI3K/mTOR, we built a 2D mTOR-SAR model that predicted the bioactivity of AKT and PI3K inhibitors towards mTOR. The interaction of the best inhibitors was evaluated by docking analysis and compared to that of the standard AZ8055 and XL388 inhibitors.

Results: A mechanistic target of rapamycin-quantitative structure-activity relationship (mTOR-QSAR) model with a correlation coefficient (R^2) of 0.80813 and a root mean square error of 0.17756 was obtained, validated and evaluated by a cross-validation leave-one-out method. The best predicted AKT and PI3K inhibitor pIC50 activities were 9.36–9.95 and 9.23–9.87 respectively.

Conclusions: After docking and several comparisons, the inhibitors with better predictions showed better affinity and interaction with mTOR compared to AZ8055 and XL388, so we have found that 2 AKT inhibitors and 9 mTOR inhibitors met the Lipinski and Veber criteria and could be future drugs.

Key words: QSAR, virtual screening, PI3K/AKT/mTOR, docking, dual ATP inhibitors.

Contemp Oncol (Pozn) 2023; 27 (3): 155–162
DOI: <https://doi.org/10.5114/wo.2023.133709>

Virtual docking screening and quantitative structure-activity relationship studies to explore AKT and PI3K inhibitors acting on mTOR in cancers by theoretical biology and medical modeling

Ilham Kandoussi^{1,2}, Hanane Abbou^{1,2}, Ghyslaine EL Haddoumi^{1,2},
Mariam Mansouri^{1,2}, Lahcen Belyamani¹⁻³, Azeddine Ibrahim^{1,2}

¹Biotechnology Laboratory (MedBiotech), Bioinova Research Center, Rabat Medical & Pharmacy School, Mohammed V University in Rabat, Morocco

²Centre Mohammed VI de la Recherche et de l'Innovation, Rabat, Morocco

³Emergency Department, Military Hospital Mohammed V, Rabat, Morocco

Introduction

The phosphatidylinositol 3-kinase (PI3K)/AKT/mechanistic target of rapamycin (mTOR) signaling pathway dominates a wide range of cellular processes including survival, proliferation, and growth, is regulated by many signaling proteins upstream and regulates many effectors downstream. This pathway is hyperactivated or altered in many types of cancer [1].

mTOR is a serine/threonine kinase that acts through two structurally and functionally distinct protein complexes, the mTOR1 complex (mTORC1) and the mTOR 2 complex (mTORC2), to detect and integrate multiple intracellular and environmental signals [2, 3].

It is excessively over-activated in more than 70% of cancers [4]. In recent years, it has been widely demonstrated in animal models and cancer patients that mTOR dysfunction contributes to tumorigenesis [5]. Thus, the components of the mTOR pathway are among the most frequently mutated genes in cancer [6].

Several types of mTOR inhibitors, such as rapamycin, its rapalogs and mTORC1/2 kinase inhibitors, have been studied in various cancer models, including breast cancer, lung cancer, colorectal cancer, and others. However, the effects of mTOR inhibitors used as monotherapy in cancer are sometimes mitigated by several mechanisms of resistance [7].

Rapamycin is an allosteric inhibitor of mTOR and has been approved as an immunosuppressant, but interest is focused on its anticancer potential. However, the performance of rapamycin and its analogs (rapalogs) has not been distinguished despite isolated success in subsets of cancers, suggesting that the full therapeutic potential of mTOR targeting has not yet been exploited. A new generation of competitive adenosine triphosphate (ATP) inhibitors that directly target the mTOR catalytic site exhibits potent and complete inhibition of mTOR and is in early clinical trials [8].

Therefore, new therapeutic strategies based on mTOR inhibition need to be further developed, including combination therapies targeting other pathway inhibitors [9]. Inhibition of the PI3K/AKT/mTOR pathway increases antitumor activity [10]. Studies have shown that the combination of compounds simultaneously targeting different molecules of the PI3K/AKT/mTOR pathway leads to synergistic activity [11].

Computational design has indeed become a powerful and essential tool in drug discovery, especially in the context of developing dual-targeted drugs

for novel kinase targets. Kinases are enzymes involved in various cellular processes and have been implicated in many diseases, including cancer. Designing drugs that can target multiple kinases simultaneously can offer significant advantages in terms of therapeutic efficacy [12].

Based on these results, we provide an *in silico* strategy for the exploration of competitive dual PI3K/mTOR and AKT/mTOR inhibitors of ATP, after two previous explorations of AKT/PI3K and mTOR/PI3K inhibitors, and PI3K/AKT and mTOR/AKT inhibitors [13, 14].

The marked interest in the development of new PI3K/AKT and PI3K/mTOR inhibitors as potential agents for cancer treatment has prompted us to explore the possibility of developing these inhibitors on the basis of quantitative structure-activity relationship (QSAR) models to predict bioactivity of PI3K and AKT inhibitors towards mTOR and the interaction of the best will be evaluated by docking analysis.

Material and methods

Dataset generation

Mechanistic target of rapamycin inhibitors were taken from Binding DataBase (<https://www.bindingdb.org>) and their IC_{50} (concentration of molecules causing 50% inhibition) was converted to a logarithmic scale, pIC_{50} . A total of 170 chemically different compounds with high activity with pIC_{50} greater than 8 were recruited to construct the mTOR-QSAR model. AKT and PI3K inhibitors with a pIC_{50} greater than 8 were also selected with the aim of predicting their activity towards mTOR using the developed QSAR model and exploring their dual activity. Compounds of significant activity were chosen to predict future effective dual inhibitors.

Quantitative structure-activity relationship model generation

184 2D descriptors available on the MOE 2008.10 (obtained from Chemical Computing Group (CCP); Montreal, QC, Canada) [15] were calculated for the 170 compounds. Invariant and insignificant descriptors were initially eliminated; then the QSAR contingency descriptor selection and intercorrelation matrices between descriptor pairs were used to extract the 52 most relevant molecular descriptors, which were employed for the distance calculation of each database entry.

All 170 selected compounds were distributed randomly to a training set with 128 compounds (75% of the data) and a test set consisting of 42 compounds (25% of the data).

Partial least squares (PLS) analysis based on the leave-one-out (LOO) method was used to correlate molecular descriptors with pIC_{50} values.

Quantitative structure-activity relationship model validation

The internal validation procedure evaluates the relative predictive performance of the QSAR model, firstly via the correlation coefficient (R^2), which is used to measure the correlation between the experimental pIC_{50} and the predicted interest values with the purpose of observ-

ing the variability between the variables in the set test, and secondly by the root mean square error (RMSE), which is used to evaluate the relative error of the QSAR model.

The model is also tested by cross-validation using the LOO method and the computation of the correlation coefficient (R^2) and mean squared error (RMSE), while the detection of outliers was conducted using Z-Score, Z -SCORE (absolute difference between the value of the model and the activity field, divided by the square root of the mean square error of the data set) and XZ -SCORE (absolute difference between the value of the model under a leave-one-out cross validation scheme and the activity field, divided by the square root of the mean square error of the data set).

External validation evaluates the activities of the predictions and the calculation of the numerical parameters using the model.

Activity prediction

The constructed and validated QSAR-mTOR model was used to predict the activity of two groups of AKT and PI3K inhibitors against mTOR, a first one being AKT inhibitors and second one being PI3K inhibitors. These inhibitors, retrieved from the Binding database (<https://www.bindingdb.org>), have a pIC_{50} greater than 8 with 578 inhibitors for AKT and 477 inhibitors for PI3K.

After calculating the predicted activity, the 40 inhibitors with the best predictions in each group were selected for docking into mTOR in order to explore their dual activity.

Molecular docking

The 3D coordinates of the PI3K inhibitors as well as AKT that showed the best predicted activity in the QSAR-mTOR model were generated from 2D by MarvinView 5.4.1.1. For the docking analysis, 4JT6 (PDB ID), the mTOR crystallized structure recovered from the PDB database with a resolution of 3.6 Å was used. For docking studies mutual graph learning (MGL) tools 1.5.6 with AutoGrid4 and AutoDock vina (Scripps) [16] were used. The mTOR structure was hydrogenated using MGL tools and PyMol was used to visualize the results [17].

In this study we followed the same docking strategy used by the authors in previously published studies [18]. The Grid boxes were generated, using MGL tools 1.5.6, around the active site of the two 3D structures of the mTOR kinase protein. The Grid boxes were set to have 16 to 20 Å of edge with coordinates $x = 49.037$, $y = -0.839$, $z = -45.349$. These coordinates were determined using the potential substrate binding residues as centroids (in the hinge region and the activation loop) [19].

AZD8055 and XL388 are known mTOR inhibitors and were also docked to mTOR to serve as a control to evaluate the docking results. Their 3D structures were obtained from PubChem.

Results

Quantitative structure-activity relationship analysis

The mTOR-QSAR model was built based on 52 molecular descriptors; the validation procedure evaluates

the predicted activities and the residuals for the molecules in the training set. In cross-validation, the model is tested using a LOO method. An mTOR-SAR model with a correlation coefficient (R^2) of 0.80813 and an RMSE of 0.17756 was obtained after the QSAR regression analysis of 170 molecules. It was validated and evaluated by the cross-validation method LOO. The predictive performance of this model was represented by cross-validated RMSE with 0.54236 and R^2 with cross-validation of 0.65460.

Figure 1 presents the plot of both the experimental and the predicted inhibitory potency pIC_{50} values of the training and test set compounds, showing a comparable and similar distribution between the two groups. No outliers were detected in the test set data, and all compounds were well-predicted with a residual value less than one log unit.

Virtual screening

The mTOR-QSAR model developed and validated was used to calculate the predicted activity of AKT and PI3K inhibitors against mTOR. Then, the 40 inhibitors with the best predictions in each group were chosen to perform their docking into mTOR. The best predicted AKT and PI3K inhibitors present pIC_{50} activities in the range 9.36–9.95 and 9.23–9.87, respectively.

Molecular docking studies

The docking scores (affinity) obtained from the docking of AKT inhibitors and PI3K inhibitors in the catalytic site of mTOR were between -7.6 and -9.6 kcal/mol for the AKT inhibitor group and between -3.0 and -10.6 kcal/mol for the PI3K inhibitor group. The mTOR reference inhibitors AZD8055 and XL388 presented score of -7.2 and -8.6 kcal/mol, respectively (Tables 1, 2).

Discussion

The PI3K/AKT/mTOR pathway is stimulated by numerous growth factors and their receptors, and it regulates metabolism, growth, survival, cell proliferation, and angiogenesis.

This pathway is one of the most frequently mutated pathways in cancer, leading to cancer progression and induces resistance to existing treatments. Combination inhibition of PI3K/AKT/mTOR signaling pathways is an approach to overcome the acquisition of resistance to cancer treatment.

In order to explore new common inhibitors of AKT/mTOR and PI3K/mTOR, an mTOR2D-QSAR model was constructed to predict the activity of one group of AKT inhibitors and another one of PI3K, then docking of those that had the best prediction (the top 40 in each group), whose results were compared to those of AZD8055 and XL388, was performed.

The mTOR inhibitors used to construct the QSAR model and those of AKT and PI3K whose activity towards mTOR was predicted were extracted from Binding Database and selected according to their IC_{50} bioactivity. The model was built by the PLS method using MOE software.

The AKT and PI3K inhibitor docking score compared to the AZD8055 and XL388 score predicts that the AKT in-

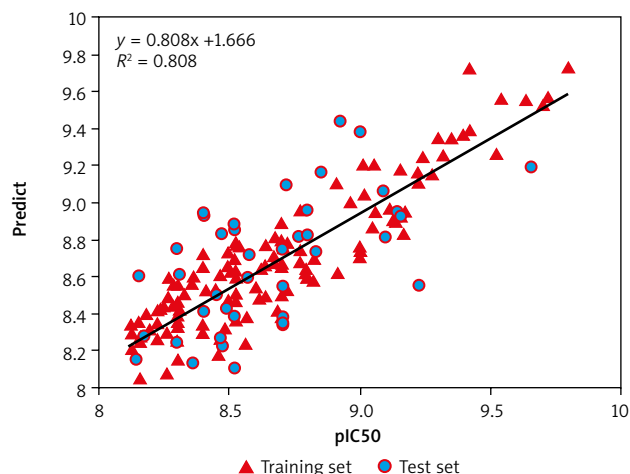


Fig. 1. Relationship between observed and predicted data from QSAR-mTOR model. The compounds of the training set are in red and those of the test set are in blue

hibitors have an affinity between -7.6 and -9.8 kcal/mol and those of PI3K have an affinity between -3.0 and -10.6 kcal/mol, while AZD8055 and XL388 have affinities of only -7.8 and -8.6 kcal/mol, respectively. Therefore 39 AKT inhibitors and 30 PI3K inhibitors had an affinity higher than that of AZD8055, and 17 AKT inhibitors and 22 PI3K inhibitors had a higher affinity than that of XL388. Thus, the affinity and interaction of XL388 would be more effective than that of AZD8055.

Visualization of these interactions showed that the different compounds adapt to the ATP binding site forming hydrogen bonds, in particular with the residue V2240, which is considered as a hinge residue for mTOR. The best inhibitor of AKT and that of PI3K establish respectively 5 and 7 hydrogen bonds with mTOR, compared to AZ8055 and XL388, which have only 3 and 4 connections, respectively. The significant affinity score of some inhibitors despite the low number of hydrogen bonds can be explained by the hydrophobic interactions and that of van der Waals. Thus, the affinity and interaction of XL388 and most of the inhibitors studied are more efficient than those of AZ8055, a potent, selective and oral mTOR kinase inhibitor, which inhibits the proliferation of tumor cells *in vitro* and *in vivo* [20], but induces apoptosis [21].

A double comparison of the inhibitors studied with respect to XL388, in consideration of the affinity and the number of mTOR-mediated hydrogen bonds, predicts that 3 AKT inhibitors (Table 3) and 10 PI3K inhibitors (Table 4) have better results than XL388.

Taking into account the modified Lipinski rules (no more than 5 hydrogen bond donors, no more than 10 hydrogen bond acceptors, an octanol-water partition coefficient $\log P$ not greater than 5.5) and the Veber rule determining good bioavailability (polar surface area ≤ 140 Å (absolute polarity measurement), rotatable bonds ≤ 10 (flexibility measurement)), we found that 2 AKT inhibitors (Table 5), of which 51061496 is the most relevant (5 hydrogen bonds and an affinity of -9.7 kcal/mol), and 9 PI3K inhibitors (Table 6), with 50291199 being the most relevant (5 hydrogen bonds and an affinity of -9.4 kcal/mol), met all the criteria and could be future drugs (Fig. 2). XL388 inhibits

Table 1. Docked interaction analysis of AKT inhibitors screened into mTOR

BindingDBReactant_set_id	pIC50	Weight	Predicted mTOR pIC50	Number of H bonds	Active site residues and bond length in Å	Affinity [–kcal/mol]
44988	8.397	559.701	9.749	4	3.4–3.4 Y2226/3.1 W2239/3.2 K2171	9.8
329800	8.167	529.586	9.533	2	3.3 E2190/3.5 D2357	8.4
329813	8.102	503.547	9.429	2	3.0 S2165/3.2 Q2166	8.3
329826	8.397	547.601	9.544	2	3.0 S2165/3.1 Q2166	8.2
329831	8.318	517.575	9.637	3	3.3 S2165/2.9 Q2166/3.6 E2190	8.7
329838	8.161	555.583	9.407	5	3.3 R2348/3.3–3.4 D2252/3.4–3.2 R2251	8.9
329842	8.387	533.573	9.410	2	3.4 D2357/3.1 T2245	8.2
329843	8.180	587.544	9.700	2	3.5 D2357/3.3 N2343	8.1
329866	8.657	551.414	9.718	2	3.3 Q2167/3.4 V2240	8.4
329867	8.552	587.875	9.941	2	3.3 V2240 /3.2 R2251	8.0
329879	8.180	477.509	9.441	3	3.3 S2342/3.4 R2251/3.3 V2240	8.3
329906	8.823	525.377	9.853	2	3.4 V2240 /3.3 Q2166	8.3
329911	8.677	474.535	9.407	2	3.4 G2238/3.0 R2251	7.6
329912	8.853	480.925	9.418	2	3.4 V2240 /3.3 Q2167	8.2
329913	8.443	506.963	9.391	2	3.4 V2240 /3.3 Q2167	8.2
329948	8.119	531.601	9.700	2	3.1 S2165/3.3 Q2166	8.3
329949	8.657	537.992	9.718	2	3.2 S2165/3.2 Q2166	8.4
329950	8.522	536.002	9.742	3	2.8 V2240 /3.3 Q2167/3.1 S2165	9.0
329958	9	523.966	9.568	2	3.2 Q2167/3.2 S2165	8.6
329959	8.638	583.609	9.471	2	3.3 Q2165/3.1 S2165	9.6
329960	8.376	515.558	9.385	2	3.4 S2342/3.4 T2245	9.1
329966	8.769	532.437	9.531	2	3.1 Q2167/3.2 S2165	8.7
329967	8.537	514.446	9.413	2	3.2 Q2167/3.1 S2165	8.3
329968	8.229	514.446	9.413	2	3.1 Q2167/3.3 S2165	8.5
329970	8.387	517.575	9.553	2	3.4 S2165/3.4 D2243	8.4
330002	8.309	524.088	9.516	2	3.2 S2165/3.1 Q2167	8.1
330007	8.376	564.453	9.957	2	3.4 S2165/3.3 D2243	8.4
330008	8.744	548.891	9.697	2	3.2 S2165/3.1 Q2167	8.6
330020	8.136	543.612	9.834	1	3.2 R2251	8.7
330052	8.638	542.584	9.491	2	3.0–3.0 T2245	9.3
330121	9.096	542.584	9.438	2	3.3 R2252/3.3 R2349	9.5
50152163	9	461.428	9.835	3	3.5–3.1 R2251/3.2 D2252	7.9
50152170	8.522	523.377	9.446	2	3.2 R2251/3.4 E2190	8.0
50197665	8.301	466.540	9.440	1	2.9 Y2225	9.5
50212679	8.221	466.540	9.440	1	3.1 S2165	8.5
50414691	8.337	466.540	9.440	1	3.0 Y2225	9.5
50426806	8.920	466.540	9.440	2	3.6 G2236/3.4 T2245	8.8
50453767	9	461.428	9.835	2	3.3 D2252/3.5 R2251	7.8
50453775	8.698	523.377	9.360	2	3.5 R2251/3.4 D2252	8.0
51061496	8.283	429.452	9.466	5	3.1 Q2167/3.1 S2165/2.8 E2190/3.2 D2357/2.9 V2240	9.7
AZD8055	9.096	465.5	*****	3	3.1 V2240 /2.8 S2165/2.9 Q2167	7.8
XL388	8.004	455.5	*****	4	3.0 Q2167/3.3 D2357/3.2 Y2225/2.5 D2195	8.6

Docking (affinity) scores of AKT inhibitors in the catalytic site of mTOR were set between –7.6 and –9.8 kcal/mol. AZ8055 and XL388 (mTOR reference inhibitors) showed scores of –7.8 and –8.6 kcal/mol.

Table 2. Docked interaction analysis of PI3K inhibitors screened into mTOR

BindingDBReactant_set_id	pIC50	Weight	Predicted mTOR pIC50	Number of H bonds	Active site residues and bond length in Å	Affinity [–kcal/mol]
45312	8.508	478.327	9.595	4	3.0 K2166/2.8 S2165/3.3 D2167/3.2 Y2225	8.2
45318	9.522	454.304	9.429	3	3.0 T2245/3.0 T2245/3.4 V2240	3.4
45347	8.744	464.299	9.638	3	3.3 Y2225/3.1–3.1 T2245	8.8
228339	8.698	444.56	9.394	4	3.5 D2357/3.4 Y2225/3.2 E2190/3.4 D2243	8.7
228340	8.301	430.532	9.234	4	3.0 E2190/3.4 Q2167/3.4 D2357/3.4C2243	8.6
228341	8.301	414.534	9.430	3	3.4 C2243/3.5 D2357/3.1 E2190	8.1
234983	9.318	360.420	9.243	3	2.9–3.4 V2240 /3.4 2190	10.1
235016	8.795	390.446	9.344	3	2.9 S2160/3.0 Q2167/3.2 N2343	8.8
235024	8.795	413.453	9.383	3	3.0 V2240 /2.9 E2190/3.2 D2357	9.6
235090	8.698	352.397	9.319	5	3.4 Q2167/3.0 S2165/3.3 D2357/2.9–2.8 Y2225	7.9
235091	8.508	348.449	9.391	2	3.4–3.1 V2241	9.7
235103	8.638	382.423	9.411	3	3.3 V2240 /3.2 Y2225/3.3 D2357	9.7
235120	8.274	426.476	9.418	5	3.2 Q2165/3.1–3.1 S2165/3.1 T2245/3.2 R2251	8.0
235121	8.585	443.479	9.233	3	2.9 T2245/2.9 S2342/3.0 Q2167	8.7
279460	8.301	467.515	9.544	2	3,0 Q2167/2.9 S2165	8.4
50196628	8.318	462.461	9.786	3	3.1 V2240 /3.3 Q2243/3.2 S2342	7.5
50196640	8.318	432.435	9.732	3	3.5 D2357/3.3 E2190/3.0 V2240	3.0
50196659	8.698	476.487	9.444	2	3.2 T2245/3.3 S2342	7.3
50196675	8.568	461.472	9.507	1	3.0 V2240	8.8
50196677	8.568	447.445	9.447	3	3.0 Q2167/3.1 S2342/3.4 V2240	8.7
50291199	8.443	458.449	9.818	5	3.3 D2357/3.3 E2190/3.2 Q2167/3.5–2.9 V2240	9.4
50291211	8.161	462.941	9.649	5	2.9–3.4 V2240 /3.5 Q2167/3.4 E2190/3.4 D2357	9.1
50291212	8.107	423.457	9.296	4	3.1 S2165/3.2–3.1 Y2225/3.3 D2195	7.5
50342300	9.638	515.951	9.305	4	3.5 E2190/3.3 Y2225/3.4 D2357/3.4 V2240	10.6
50342352	10.154	520.520	9.561	3	3.1 Q2167/2.9 S2165/3.1 G2238	9.0
50563173	8.958	504.639	9.508	7	3.0–2.9–3.4 S2165/3.4 K2166/3.2–3.1 D2167/3.3 V2240 /3.3 D2244	8.1
50570923	8.221	650.705	9.406	3	3.4 Y2225/3.0 R2347/3.3 D2252	7.9
50571373	9.000	435.532	9.830	4	3.3 V2240 /3.0–3.1 Q2167/2.9 S2165	7.4
50623515	8.221	366.389	9.377	4	3.4 D2357/3.4 N2343/3.3 V2240 /3.1 T2245	7.6
50698327	8.537	433.418	9.483	4	3.1 V2240 /G2238 3.2/3.6 T2245/3.2 Q2167	9.2
50703936	8.698	490.613	9.531	7	3.0–3.2 D2243/3.1 V2240 /3.1 S2342	7.4
50717323	8.522	513.646	9.261	4	3.5–2.9 V2240 /3.1 S2342/3.1 H2247	9.0
50919348	8.522	537.547	9.879	4	3.0 Y2225/3.5 D2357/3.1 D2167/2.9 S2165	9.5
50927440	8.657	468.442	9.493	2	3.1 V2240 /3.2 T2244	8.9
51028203	8.283	508.006	9.655	5	2.8 V2240 /3.2 D2357/3.0 D2195/3.5 Y2224/2.9 R2251	8.9
51045941	8.221	417.419	9.286	1	3.1 Q2167	8.9
51065315	8.537	445.405	9.761	4	3.1–3.5 V2240 /3.2 T2245/3.1 R2251	7.3
51092393	8.468	457.461	9.596	5	2.9–3.5 V2240 /3.4 D2357/3.3 Q2167/3.2 E2190	9.4
51092412	8.619	615.657	9.554	5	3.3 V2240 /3.3 D2243/3.0 R2348/3.0 S2165/3.2 D2167	3.2
AZD8055	9.096	465.5	*****	3	3.1 V2240 /2.8 S2165/2.9 Q2167	7.8
XL388	8.004	455.5	*****	4	3.0 Q2167/3.3 D2357/3.2 Y2225/2.5 D2195	8.6

Docking (affinity) scores of PI3K inhibitors in the catalytic site of mTOR were set between –3.0 and –10.6 kcal. AZ8055 and XL388 (mTOR reference inhibitors) showed scores of –7.8 and –8.6 kcal/mol.

Table 3. Comparison of AKT inhibitors studied to XL388

BindingDBReactant_set_id	Weight	Predicted mTOR pIC50	HB	AFFINITY [–kcal/mol]	b_rotN	a_acc	a_don	SlogP	TPSA
44988	559.701	9.749	4	9.8	6	7	1	6.001	111.53
329838	555.583	9.407	5	8.9	7	6	3	5.137	104.78
51061496	429.452	9.466	5	9.7	5	6	2	2.074	123.69

AKT inhibitors with better affinity and number of hydrogen bonds than XL388

Table 4. Comparison of PI3Kinhibitors studied to XL388

BindingDBReactant_set_id	Weight	Predicted mTOR pIC50	HB	AFFINITY [–kcal/mol]	b_rotN	a_acc	a_don	SlogP	TPSA
228339	444.56	9.394	4	8.7	7	6	2	1.711	123.33
228340	430.532	9.234	4	8.6	6	6	3	1.056	134.33
50291199	458.449	9.818	5	9.4	5	6	2	3.065	132.98
50291211	462.941	9.649	5	9.1	5	6	2	3.501	132.98
50342300	515.951	9.305	4	10.6	5	6	1	5.547	97.730
50698327	433.418	9.483	4	9.2	4	7	1	1.622	101.66
50717323	513.646	9.261	4	9.0	5	8	2	2.414	107.55
50919348	537.547	9.879	4	9.5	7	7	4	4.970	132.22
51028203	508.006	9.655	5	8.9	5	8	1	0.213	135.07
51092393	457.461	9.596	5	9.4	5	5	2	3.670	120.09

PI3K inhibitors with better affinity and number of hydrogen bonds than XL388

Table 5. AKT inhibitors meeting Lipinski and Veber criteria

BindingDBReactant_set_id	Name
329838	6-[4-[1-[2-(azetidin-1-yl)ethyl]-4-[4-fluoro-3-(trifluoromethyl)phenyl]imidazol-2-yl]piperidin-1-yl]-5-(1H-pyrazol-4-yl)pyrimidin-4-amine
51061496	2-amino-6-(5-fluoro-6-methoxypyridin-3-yl)-8-[4-(hydroxymethoxy)cyclohexyl]-4-methylpyrido[2,3-d]pyrimidin-7-one

AKT inhibitors with better affinity and interaction with mTOR than XL388 and meeting Lipinski and Veber criteria

Table 6. PI3K inhibitors meeting Lipinski and Veber criteria

BindingDBReactant_set_id	Name
228339	N-[5-[2-[2-amino-4-ethyl-6-(4-methoxypiperidin-1-yl)pyrimidin-5-yl]ethynyl]-2-methylpyridin-3-yl]methanesulfonamide
228340	N-[5-[2-[2-amino-4-ethyl-6-(4-hydroxypiperidin-1-yl)pyrimidin-5-yl]ethynyl]-2-methylpyridin-3-yl]methanesulfonamide
50291199	N-[5-(2-amino-4-methylpyrido[2,3-d]pyrimidin-6-yl)-2-methoxypyridin-3-yl]-2,4-difluorobenzenesulfonamide
50291211	N-[5-(2-amino-4-methylpyrido[2,3-d]pyrimidin-6-yl)-2-methoxypyridin-3-yl]-5-chlorothiophene-2-sulfonamide
50698327	2-(difluoromethyl)-1-(4,6-dimorpholin-4-yl-1,3,5-triazin-2-yl)benzimidazol-4-ol
50717323	4-[2-(1H-indazol-4-yl)-6-[(4-methylsulfonylpiperazin-1-yl)methyl]thieno[2,3-d]pyrimidin-4-yl]morpholine
50919348	N-[2-amino-5-[3-(3,4-dimethoxyphenyl)-1H-pyrrolo[2,3-b]pyridin-5-yl]pyridin-3-yl]-2,4-difluorobenzenesulfonamide
51028203	5-[5-chloro-2-[(4-methylsulfonylpiperazin-1-yl)methyl]-8-morpholin-4-ylimidazo[1,2-a]pyrazin-6-yl]pyrimidin-2-amine
51092393	N-[5-(2-amino-4-methylquinazolin-6-yl)-2-methoxypyridin-3-yl]-2,4-difluorobenzenesulfonamide

PI3K inhibitors with better affinity and interaction with mTOR than XL388 and meeting Lipinski and Veber criteria

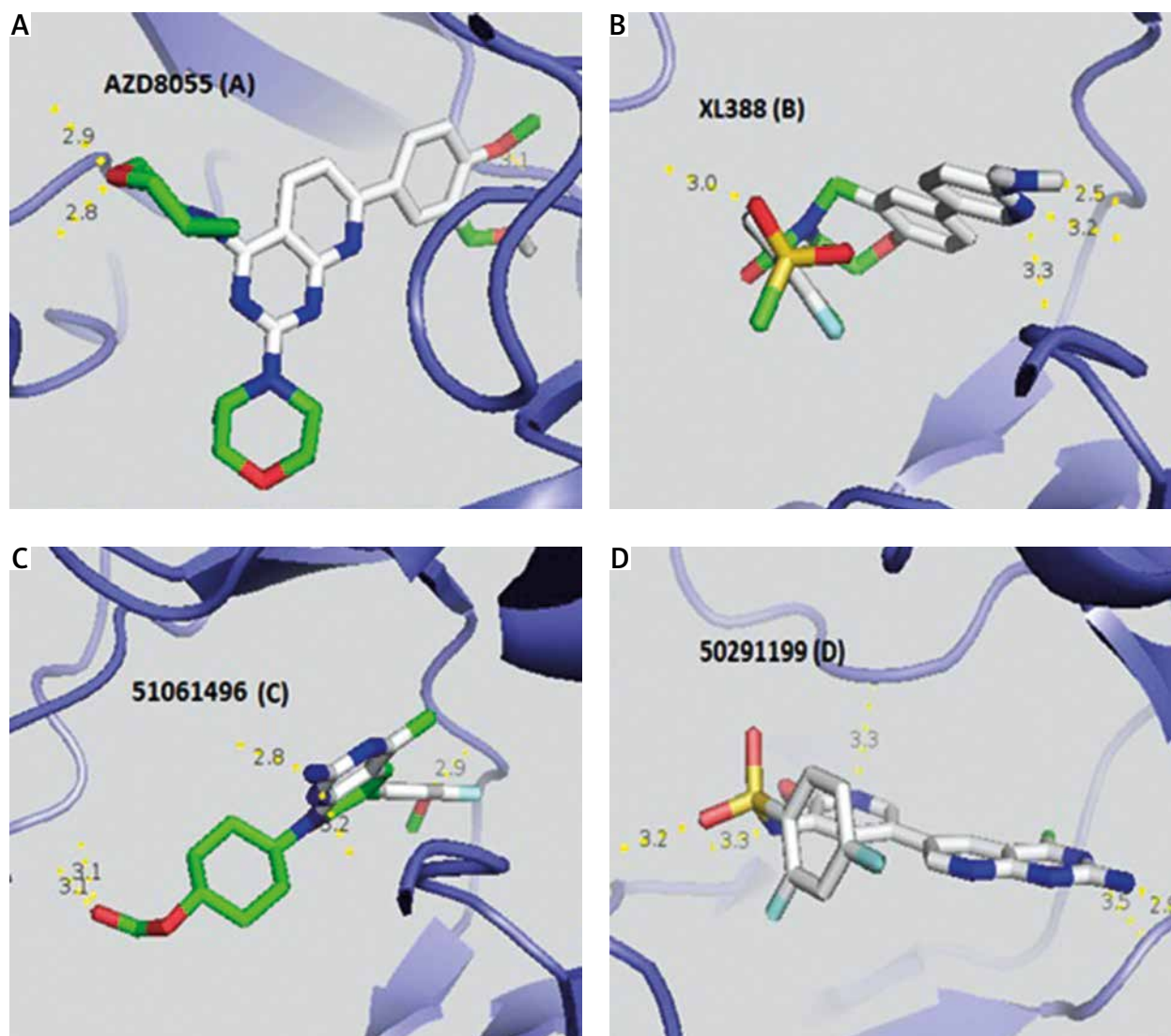


Fig. 2. Visualization of the different interactions between the compounds and the active site of mTOR via the hydrogen bonds. AZD8055 (A) and XL388 (B) respectively have 3 and 4 linkages with the catalytic site of mTOR whereas 51061496 inhibitor of AKT (C) and 50291199 inhibitor of PI3K (D) both have 5 hydrogen bonds

Red zones – oxygen atom, blue zones – nitrogen atom, green zones – other. Hydrogen bonds are represented by a dashed yellow line. Numbers represent the size of the hydrogen bonds established between the ligand and the receptor.

the survival and proliferation of certain cell lines and blocks activation of the mTORC1 and mTORC2 complex [22].

Conclusions

The hyperactivation of the PI3K/AKT/mTOR pathway in cancer, in association with the crucial role of mTOR signaling in tumorigenesis, has led to considerable efforts to generate inhibitors to target this pathway. Using a QSAR model, we were able to predict the activity of the powerful AKT and PI3K inhibitors towards mTOR, select the best ones and analyze their interaction with mTOR by docking while comparing them to a reference mTOR inhibitor. Promising results were obtained, and the dual inhibitors AKT/mTOR and PI3K/mTOR were predicted, pending the testing of these compounds directly on cancer cell lines in our next study.

Acknowledgments

This work was carried out with national funding from the Moroccan Ministry of Higher Education and Scientific Research (PPR program) to AI.

The authors declare no conflict of interest.

References

1. Ersahin T, Tuncbag N, Cetin-Atalay R. The PI3K/AKT/mTOR interactive pathway. *Mol Biosyst* 2015; 11: 1946-1954.
2. Laplante M, Sabatini DM. mTOR signaling in growth control and disease. *Cell* 2012; 149: 274-293.
3. Saxton RA, Sabatini DM. mTOR signaling in growth, metabolism, and disease. *Cell* 2017; 168: 960-976.

4. Forbes SA, Bindal N, Bamford S, et al. COSMIC: mining complete cancer genomes in the Catalogue of Somatic Mutations in Cancer. *Nucleic Acids Res* 2011; 39: D945-D950.
5. Ciuffreda L, di Sanza C, Incani UC, Milella M. The mTOR pathway: a new target in cancer therapy. *Curr Cancer Drug Targets* 2010 ; 10 : 484-495.
6. Mayer IA, Arteaga CL. The PI3K/AKT pathway as a target for cancer treatment. *Ann Rev Med* 2016 ; 67 : 11-28.
7. Faes S, Demartines N, Dormond O. Resistance to mTORC1 inhibitors in cancer therapy: from kinase mutations to intratumoral heterogeneity of kinase activity. *Oxid Med Cell Longev* 2017;2017:1726078.
8. Benjamin D, Colombi M, Moroni C, et al. Rapamycin passes the torch: a new generation of mTOR inhibitors. *Nat Rev Drug Discov* 2011; 10: 868-880.
9. Tian T, Li X, Zhang J. mTOR signaling in cancer and mTOR inhibitors in solid tumor targeting therapy. *Int J Mol Sci* 2019; 20: 755.
10. Vivanco I, Sawyers CL. The phosphatidylinositol 3-kinase-AKT pathway in human cancer. *Nat Rev Cancer* 2002; 2: 489.
11. Polivka J, Janku F. Molecular targets for cancer therapy in the PI3K/AKT/mTOR pathway. *Pharmacol Ther* 2014; 142: 164-175.
12. Sun D, Zhao Y, Zhang S, et al. Dual-target kinase drug design: current strategies and future directions in cancer therapy. *Eur J Med Chem* 2020; 188: 112025.
13. Kandoussi I, Benharrif O, Lakhlili W, et al. Virtual docking screening and QSAR studies to explore AKT and mTOR inhibitors acting on PI3K in cancers. *Contemp Oncol (Poznan)* 2020; 24: 5-12.
14. Kandoussi I, Benharrif O, Lakhlili W, et al. Virtual docking screening and QSAR studies to explore PI3K and mTOR inhibitors acting on AKT in cancers. *J Cancer Sci Clin Ther* 2021; 5: 35-48.
15. Vilar S, Cozza G, Moro S. Medicinal chemistry and the molecular operating environment (MOE): application of QSAR and molecular docking to drug discovery. *Curr Top Med Chem* 2008; 8: 1555-1572.
16. Trott O, Olson AJ. AutoDock Vina: improving the speed and accuracy of docking with a new scoring function, efficient optimization and multithreading. *J Comput Chem* 2010; 31: 455-461.
17. Seeliger D, de Groot BL. Ligand docking and binding site analysis with PyMOL and Autodock/Vina. *J Comput Aided Mol Des* 2010; 24: 417-422.
18. Lakhlili W, Chev e G, Yasri A, et al. Determination and validation of mTOR kinase-domain 3D structure by homology modeling. *OncoTargets Ther* 2015; 8: 1923-1930.
19. Lakhlili W, Yasri A, Ibrahimi A. Structure-activity relationships study of mTOR kinase inhibition using QSAR and structure-based drug design approaches. *OncoTargets Ther* 2016; 9: 7345-7353.
20. Chresta CM, Davies BR, Hickson I, et al. AZD8055 is a potent, selective, and orally bioavailable ATP-competitive mammalian target of rapamycin kinase inhibitor with *in vitro* and *in vivo* antitumor activity. *Cancer Res* 2010; 70: 288-298.
21. Cirstea D, Santo L, Hideshima T, et al. Delineating the mTOR kinase pathway using a dual TORC1/2 inhibitor, AZD8055, in multiple myeloma. *Mol Cancer Ther* 2014; 13: 2489-2500.
22. Xiong Z, Zang Y, Zhong S, et al. The preclinical assessment of XL388, a mTOR kinase inhibitor, as a promising anti-renal cell carcinoma agent. *Oncotarget* 2017; 8: 30151-30161.

Address for correspondence

Ilham Kandoussi

Biotechnology Laboratory (MedBiotech)
Bioinova Research Center
Rabat Medical and Pharmacy School
Mohammed V University
Rabat, Morocco
e-mail: ilham.kandoussi.facmedecine@gmail.com

Submitted: 03.01.2023

Accepted: 04.10.2023